Journal of Electroanalytical Chemistry 835 (2019) 137–142

Contents lists available at ScienceDirect

Journal of Electroanalytical Chemistry

journal homepage: www.elsevier.com/locate/jelechem

Phytic acid@Ag-based all-solid-state ion selective electrode for potentiometric detection of Cu^{2+}

Zhenzhen Wang, Wanxin Tang, Juan Yu, Fan Zhang*, Pingang He

College of Chemistry and Molecular Engineering, East China Normal University, 500 Dongchuan Road, Shanghai 200241, PR China

ARTICLE INFO

Keywords:
All-solid-state ion selective electrodes
Phytic acid@Ag
Potentiometric detection

ABSTRACT

In this study, a novel all-solid-state ion selective electrode (ASS-ISE) was developed for the detection of Cu^{2+} by open circuit potential (OCP) based on phytic acid (PA)@Ag, which forms a thin anion layer interacting with positive charged Cu^{2+}. Due to the excellent conductivity and complexing ability with multi-chelating features, PA can selectively recognize metal ions and execute ion-electron conduction. Moreover, with the assistance of Ag nanoparticles, multiple PA molecules were connected, forming a network structure with the improved conductivity and stability. After optimizing the thickness of PA@Ag film, this ASS-ISE gave a near Nernstian behavior (31.3 ± 1.8 mV/dec) towards the variation of Cu^{2+} concentration in the range of 1.0×10^{-5} to 1.0×10^{-3} mol/L with a detection limit of 2.7×10^{-6} mol/L, and presented excellent selectivity and stability. Furthermore, it was applied in the analysis of Cu^{2+} in environmental waters with the satisfactory recoveries, and the results were consistent well with those obtained by inductively coupled plasma atomic emission spectrometer, providing a promising alternative for the on-site detection of Cu^{2+} with simplicity and reliability.

1. Introduction

Portable and reliable all-solid-state ion selective electrodes (ASS-ISEs) without any internal filling solution are highly required for potentiometric on-site and real-time monitoring of heavy metal ions. Since the original form of ASS-ISEs, the coated-wire ISEs, were came up [1], they have aroused extensive attention with the advantages of small sample volumes, simple operation and easy maintenance, and have been applied in the fields of portable [2] and wearables [3,4] devices, intelligent sensing [5,6], environmental monitoring [7,8] and so on.

Sensitive membrane is an important component of ASS-ISEs, in which ionophore plays a key role. In general, ionophores have the coordination cavity and the coordination point with suitable space arrangement [9] to recognize target ions at a high speed, forming a stable complex. However, the presence of water layer between the sensitive membrane and the electrode bulk is ubiquitous, causing the unstable potentiometric responses and further restricting the development of ASS-ISEs [10,11]. To solve this problem, many hydrophobic and conductive materials, such as micro/nanocarbon materials [12,13], polymers [14,15] and molecular redox couples [16,17], were exploited as the transition layer, also known as solid contact layer, between the sensitive membrane and the electrode. Alternatively, some novel complex, composed of ligand molecules and nanomaterials [18,19] were introduced in ASS-ISEs with the advantages of easy fabrication and high stability. The conductive metal nanomaterials acted as solid contact layer and the ligand molecules binding to the target were employed as sensitive membrane. The formation of the chemical bond between the ligand molecules and the nanomaterials can transfer the charge of the combined target ion to the electrode surface.

Phytic acid (PA, also called inositol hexaphosphate) containing six phosphates on both sides of the cyclohexane, exhibits stronger affinity for metal ions, because the cyclohexane ring has enough flexibility for the chelating and six phosphates contain multi oxygen atoms for the coordination [20]. Moreover, PA has different protonated forms, since phosphate groups could act as both proton acceptor and donor by self-dissociation, beneficial to the maintenance of electric neutral [21–24] and the further diffusion of metal ions to the electrode surface. Meanwhile, PA possesses a good conductivity [24]. Consequently, PA could serve both as a selective recognition element and an ion-to-electron transducer. However, PA has not been applied in potentiometric sensing.

In this work, PA was employed to develop a novel all-solid-state ion electrode for the potentiometric determination of Cu^{2+} with open circuit potential (OCP) technology (Scheme 1). To increase further the conductivity and stability of PA, Ag nanoparticles (AgNPs) were presented as a cross-linking agent, forming a porous network structure

* Corresponding author.
E-mail address: fzhang@chem.ecnu.edu.cn (F. Zhang).

https://doi.org/10.1016/j.jelechem.2019.01.031
Received 27 October 2018; Received in revised form 8 January 2019; Accepted 13 January 2019
Available online 16 January 2019
1572-6657/

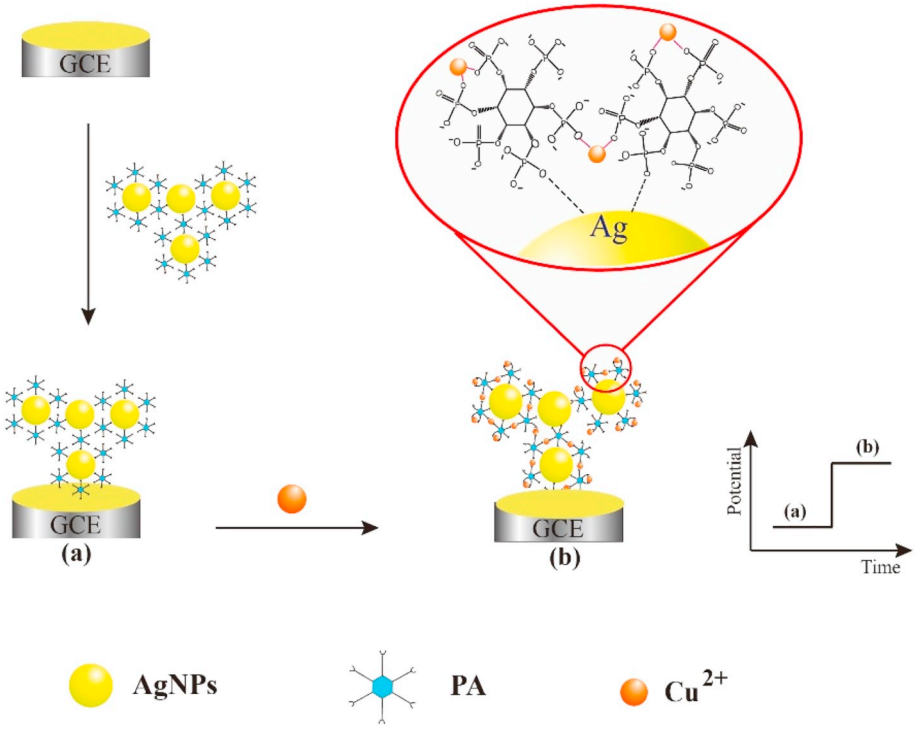

Scheme 1. Schematic diagram of the fabrication of PA@Ag modified electrode and the OCP detection of Cu^{2+}.

(PA@Ag). This complex was coated on the electrode surface to forms a thin anion layer and selectively recognized Cu^{2+}. The proposed approach may offer a simple and reliable way to fabricate ASS-ISE for the determination of metal ions in the environmental samples.

2. Experimental

2.1. Reagents

Dodecasodium of phytic acid (PA) were purchased from Sigma-Aldrich (Shanghai, China). Silver nitrate ($AgNO_3$), trisodium citrate dihydrate ($C_6H_5Na_3O_7{\cdot}2H_2O$), sodium borohydride ($NaBH_4$), acetic acid (HAc), sodium acetate (NaAc), copper chloride dihydrate ($CuCl_2{\cdot}2H_2O$), ferrous chloride tetrahydrate ($FeCl_2{\cdot}4H_2O$), calcium chloride ($CaCl_2$), magnesium chloride hexahydrate ($MgCl_2{\cdot}6H_2O$), mercury nitrate monohydrate ($Hg(NO_3)_2{\cdot}H_2O$), lead nitrate ($Pb(NO_3)_2$), manganese acetate tetrahydrate ($C_4H_6MnO_4{\cdot}4H_2O$) and zinc chloride ($ZnCl_2$) were obtained from Sinopharm Chemical Reagent Co. (Shanghai, China). Cd (II) standard solution (1 mg/mL) and Cr (III) standard solution (1 mg/mL) was purchased from Merck Serono Co., Ltd. (Shanghai, China). All reagents were of analytical reagent grade. Double distilled water ($\geq$18.2 MΩ·cm) was used throughout.

2.2. Apparatus

The open circuit potential and chronopotentiometric measurements were performed using CHI 660C electrochemical workstation (CH Instruments, Shanghai, China). AgNPs and PA@Ag were characterized with transmission electron microscope (TEM, JEOL, JEM-2100F, Japan) and Fourier transform infrared spectrometer (FTIR, Nicolet, NEXUS 670, USA). The determination of real samples was verified by inductively coupled plasma atomic emission spectrometer (ICP-AES, Thermo-Fisher, iCAP630, USA). The ultra-pure water came from Millipore Milli-Q (Shanghai, China).

2.3. Fabrication of PA@Ag-modified ASS-ISE (PA@Ag/ASS-ISE)

PA@Ag were synthesized according to a previous report with some modifications [25]. Briefly, 3 mL of 1 mmol/L PA solution was added to 100 mL of 1 mmol/L silver nitrate solute in the flask, followed by the reflux at 120 °C for 1 h to obtain PA-$AgNO_3$ mixture. Subsequently, 3 mL of 1% tri-sodium citrate was slowly added to the above solution under vigorous agitation. About 1 h later, the mixing of 1 mg/mL $NaBH_4$ resulted in the generation of PA@Ag at the concentration of 1.0 mmol/L, which were then dispersed in water and stored in the dark.

The glassy carbon electrode (GCE, d = 3 mm) was first polished using 30 nm Al_2O_3 slurry to a mirror-like surface, and then sonicated successively in ethanol and ultra-pure water for 3 min with the further drying under N_2 blowing. Subsequently, 10 μL of PA@Ag was dripped on GCE surface and dried at room temperature under dark environment, obtaining the PA@Ag/ASS-ISE.

2.4. Potentiometric measurements

The OCP determinations were performed continuously under the magnetical stirring at room temperature, when $CuCl_2$ solution at a certain concentration was successively added into the acetate buffer solution with the pH value fixed at 4.5. According to the solubility product constant of $Cu(OH)_2$ at room temperature ($K_{sp} = 2.0 \times 10^{-22}$), when the concentration of Cu^{2+} reaches 1.0×10^{-3} mol·L^{-1}, the highest value used here, pH is approximately equivalent to 4.5. Thus, it could maintain the dissolution of Cu^{2+} in all processes of determination. PA@Ag/ASS-ISE and Ag/AgCl (3 mol/L KCl) were utilized as indication electrode and reference electrode, respectively.

2.5. Chronopotentiometric measurements

A conventional three-electrode system was employed to perform the chronopotentiometric measurements, in which PA@Ag/ASS-ISE, Ag/AgCl (3 M KCl) and Pt wire were used as the working electrode, reference electrode and auxiliary electrode, respectively. The responses

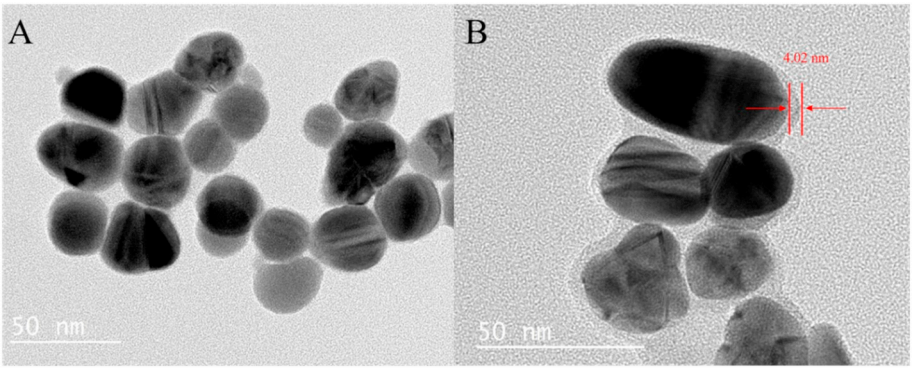

Fig. 1. TEM images of (A) AgNPs and (B) PA@Ag.

were recorded in 1 × 10^{-5} mol/L $CuCl_2$ solution, as applying a current of +1 nA for 60 s and − 1 nA for another 60 s.

3. Results and discussion

3.1. Characterization of the PA@Ag complex

TEM, FTIR and OCP were utilized to characterize the successful formation of PA@Ag complex. As shown in Fig. 1A, the synthesized AgNPs disperse evenly without aggregation and the diameter is about 30 nm. With the presence of PA, there is an obvious covering with ~4.02 nm in thickness observed on the surface of AgNPs (Fig. 1B). Fig. 2 displays the FTIR spectra of PA and PA@Ag. The absorption peaks at 1010 cm^{-1}, 1060 cm^{-1}, 1130 cm^{-1} and 1650 cm^{-1} belong to P—H banding, P—O bond in P—OH, the P═O bond in PO_4^{3-}, and the O—H bending vibration of the P—OH group, respectively [20,26]. After the combination with AgNPs, the decreased peaks at 1010 cm^{-1}, 1060 cm^{-1} are caused by the formation of P—O—Ag, and the high intensity at 3270 cm^{-1} comes from the stretching vibrations of O—H groups in H_2O. Meanwhile, the characteristic peak located at 1530 cm^{-1}, originating from the O═P—O—Ag bond, appears on the PA@Ag complex. Therefore, it can be concluded that AgNPs were covered by PA, forming the PA@Ag complex.

PA@Ag was modified on the electrode and the potentiometric responses towards Cu^{2+} at different concentrations were further investigated. From Fig. 3, it can be seen that PA@Ag/ASS-ISE presents the obvious change of potential towards Cu^{2+} in the range of 10^{-9} mol/L to 10^{-3} mol/L. PA could easily capture Cu^{2+} with the formation of chelating bond between Cu^{2+} and oxygen atoms, and be deprotonated to maintain membrane neutrality with the binding of Cu^{2+}. Thus,

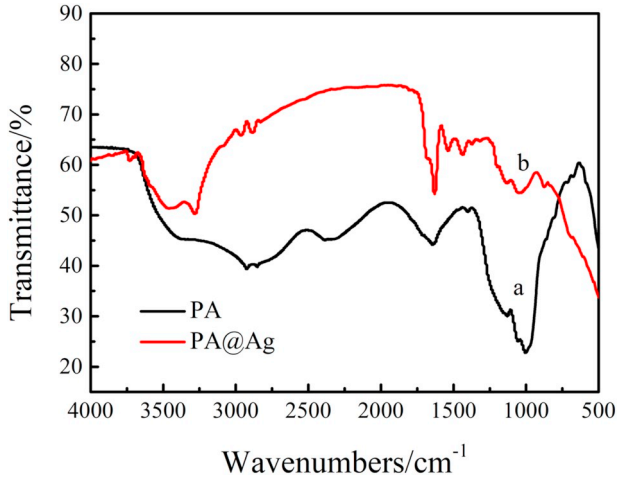

Fig. 2. FT-IR spectra of PA (a) and PA@Ag (b).

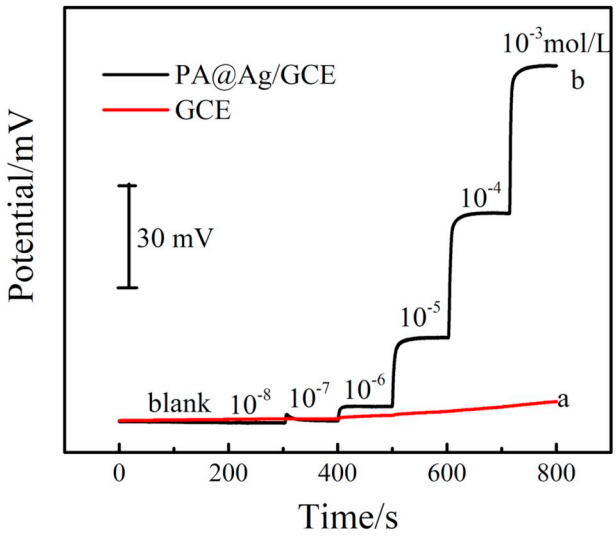

Fig. 3. Potentiometric responses towards the concentration variation of Cu^{2+} on GCE (a) and PA@Ag/ASS-ISE (b).

PA@Ag acts similarly as an ionophore in traditional ISEs. Moreover, PA@Ag is conductive and contributes to ion-electron transduction as a solid contact layer. According to P. Bühlmann's paper, the transduction mechanism may rely on a high double layer capacitance [11], provided by the large surface area. While, the responses of the bare electrode have just a little increment with the increased concentrations of Cu^2, due to the increase in ionic strength. Therefore, PA@Ag could be used to fabricate ASS-ISE for the detection of Cu^{2+}.

3.2. Optimization of the experimental conditions

In order to obtain the best performance, the thickness of PA@Ag film on the ASS-ISE was optimized. Clearly, with increasing the amount of PA@Ag from 1.5 pmol to 3.7 pmol, the linear range becomes gradually smaller (Fig. 4A). Meanwhile, the deduced slopes in Fig. 4B increase rapidly as the amount of PA@Ag increases from 0 to 1.5 pmol. While, the further increase of the amount results in a declined slope, because more PA@Ag could combine more Cu^{2+}, but overmuch PA@Ag could cause charge transfer difficulties. Moreover, 1.5 pmol of PA@Ag shows a closer change to the Nernst responses. The thickness of PA@Ag was further estimated roughly according to the diameter of PA@Ag (~30 nm) and the electrode (3 mm). Assuming that the nanoparticles are evenly dispersed on the surface of the electrode, a layer of 10^{10} PA@Ag molecules is required. 1.5 pmol of PA@Ag is equivalent to 9 × 10^{11} PA@Ag molecules, thus about 90 layers were obtained with the approximate thickness of 3 μm, closing to the thickness of the hydration layer. With this thickness, the PA@Ag modified electrode

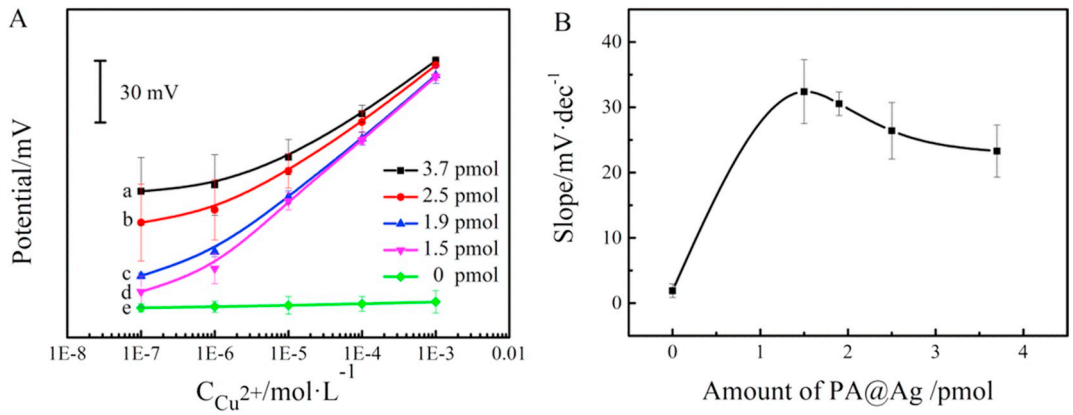

Fig. 4. (A) Potentiometric responses of PA@Ag/ASS-ISE with different amounts of PA@Ag: 3.7 pmol (a), 2.5 pmol (b), 1.9 pmol (c), 1.5 pmol (d) and 0 pmol (e). (B) Variation of slopes extracted from the potentiometric responses of PA@Ag/ASS-ISE with different amount of PA@Ag.

exhibits the best sensitivity of 31.3 mV/dec. Hence, 1.5 pmol was used as the optimal condition.

3.3. Potentiometric performance of PA@Ag/ASS-ISE

With the optimal amount of PA@Ag, the time-dependent potential responses were recorded by PA@Ag/ASS-ISE after the successive addition of Cu^{2+} to the acetate buffer (Fig. 5A). It can be observed that the potential values increase with the rising of the concentration from 1.0×10^{-9} mol/L to 1.0×10^{-3} mol/L. Correlating the potential values to the logarithm of the concentration of Cu^{2+} could obtain a linear relationship and this potentiometric responses accord with the Nernstian equation with a slope of 31.3 ± 1.8 mV/dec in the range of 1.0×10^{-5} mol/L–1.0×10^{-3} mol/L (according to the Debye-Hükel equation, when the concentration is < 0.1 mol/L, the activity and concentration are considered to be approximately equal, so the concentration was used here for plotting). The limit of detection was calculated as 2.7×10^{-6} mol/L, according to the intersection of the two slopes (Fig. 5B) [27]. In addition, the inset in Fig. 5A illustrates that the stationary time, which is defined as the time required for 90% potential change, is about 20 s. This value is much smaller than those of ISEs containing liquid membrane [28], since the thinner layer could perform a faster diffusion to electrode surface than liquid membrane. Consequently, PA@Ag/ASS-ISE exhibits high sensitivity, a wide linear range and fast response for the detection of Cu^{2+}.

3.4. Selectivity of PA@Ag/ASS-ISE

Using the separated solution method (SSM) [29], the potentiometric responses to 1.0×10^{-4} mol/L Cu^{2+} and the interfering ions were recorded and represented by E_{Cu} and E_J, respectively. The potentiometric selectivity coefficients ($\log K_{Cu,J}$) of PA@Ag/ASS-ISE were calculated using the follow equation: $\log K_{Cu,J} = \frac{(E_J - E_{Cu})Z_{Cu}F}{2.303RT} + \log\left(a_{Cu}/a^{\frac{Z_{Cu}}{Z_J}}\right)$ (a_{Cu} and a_J represent the activity of Cu^{2+} and interfering ions, respectively; Zc_u, Z_J represent the charge number of Cu^{2+} and interfering ion, respectively). The obtained value of $\log K_{Cu,J}$ means that the concentration ratio of interfering ion to Cu^{2+} for the same responses is equal to $10^{|\log K_{Cu,J}|}$. Thus, PA@Ag/ASS-ISE presents the satisfactory selectivities for most interfering ions in Table 1, probably due to the higher stability of PA/Cu^{2+} than other PA complexes [30].

3.5. Stability of PA@Ag/ASS-ISE

Due to the structural characteristics of the ASS-ISE itself, the water layer exists unavoidably between solid contact and sensitive film of the ASS-ISE. It could cause the potential drift, leading to a decrease in the stability and reproducibility of the ASS-ISE. In this work, PA@Ag is a complex, in which encapsulation of oxygen-rich PA could prevent water molecules from entering between phytic acid and silver nanoparticles. In order to verify this deduction, the water layer test was performed with immersing PA@Ag/ASS-ISE in 10^{-4} M $CuCl_2$, 10^{-2} M NaCl and 10^{-4} M $CuCl_2$ successively. According to the potentiometric responses in Fig. 6(A), the corresponding electrode drifts were calculated as 1.19 μV/s, 0.91 μV/s and 0.56 μV/s, respectively. These small values reveal the high stability of the fabricated ASS-ISE [31]. Referring the previous research [31,32], it could be concluded that the integrated PA@Ag avoids the formation of the water layer in the ASS-ISE to some extent.

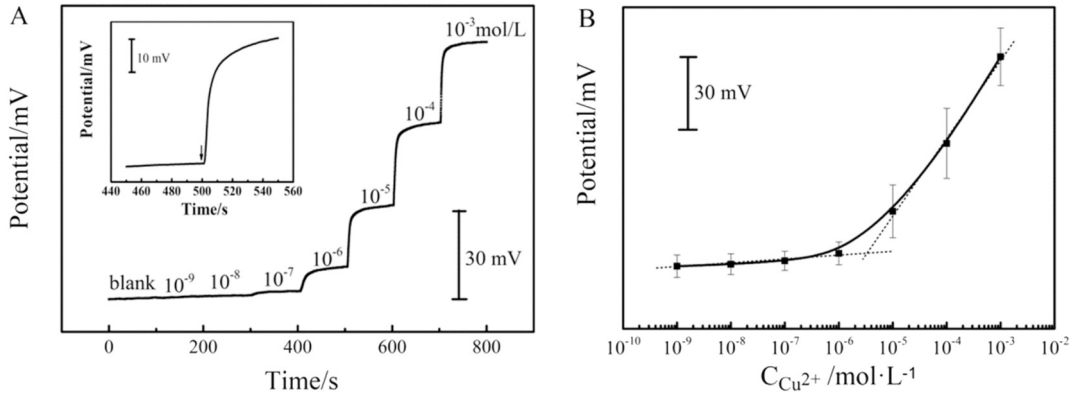

Fig. 5. (A) Time-dependent potential responses of Cu^{2+} at different concentrations on the PA@Ag/ASS-ISEs in 0.2 mol/L acetate buffer (pH = 4.5). (B) Correlation between the potential and the concentration of Cu^{2+}.

Table 1
Potentiometric selectivity coefficients, log K_{Cu}^{2+}, $_{J}$, of the PA@Ag modified electrode, obtained by the separate solution method (n = 3).

Interfering ions	$\log K_{Cu,J}^{2+}$
Cd^{2+}	−2.0 ± 0.3
Mg^{2+}	−2.3 ± 0.3
Fe^{2+}	−2.5 ± 0.6
Pb^{2+}	−2.6 ± 0.4
Cr^{3+}	−2.6 ± 0.9
Zn^{2+}	−3.1 ± 0.7
Hg^{2+}	−3.2 ± 0.7
Mn^{2+}	−4.9 ± 1.4

The stability of the PA@Ag/ASS-ISE was investigated by chronopotentiometry [33], a convenient and fast experimental technique, has been widely used to evaluate the electrical capacity and short-term potential stability of the ISEs without performing any long-term stability study. Fig. 6B shows that PA@Ag/ASS-ISEs were applied by +1 nA for 60 s and − 1 nA for another 60 s, and a potential jump appears at 60 s. This variation could be used to calculate the total resistance of the electrode. According to the equation: Potential drift = $\Delta E/\Delta t = i/C_{LF}$ (C_{LF} represents low frequency capacitance), the potential drift and capacitance were calculated as 16.7 μV/s and 6×10^{-5} F, respectively. This capacitance value was higher than the all-solid-state IESs with the separated solid contact layer and sensitive film, indicating the more excellent stability [34], because this PA@Ag/ASS-ISE was prepared by one-step process, and the formation of Ag—O between PA and AgNPs promotes the electron transfer, increasing the stability of the electrode.

Furthermore, the long term stability of PA@Ag/ASS-ISE was investigated by extracting the slopes of potential collected by this electrode and further correlating with the logarithm of concentrations (Fig. 6C). Clearly, the response slopes vary only a few millivolts over 8 days, indicating that the prepared PA@Ag/ASE have a high long term stability.

Table 2
Application of the proposed PA@Ag/ASS-ISE in the determination of Cu^{2+} in river water (n = 3).

Sample	Add ($\times 10^{-7}$ Mol/L)	Present method ($\times 10^{-7}$ Mol/L)	AAS ($\times 10^{-7}$ Mol/L)	Recovery (%) (present method)
1	0	4.4 ± 0.9	3.9 ± 1.4	–
2	10.0	13.8 ± 1.1	13.3 ± 0.8	94.0
3	30.0	34.9 ± 0.6	34.5 ± 0.8	101.7
4	50.0	56.2 ± 0.4	51.1 ± 2.2	103.6

3.6. Analysis of real samples

In order to demonstrate the feasibility in environmental monitoring, the proposed PA@Ag/ASS-ISE was employed to detect Cu^{2+} in river water. Before the detection, 1.0, 3.0, and 5.0 nM Cu^{2+} were spiked into the river water samples respectively to display the accuracy and anti-interference performance of PA@Ag/ASS-ISE. In addition, the samples were acidified with 0.2 mol/L acetate buffer (pH = 4.5) to maintain the same detection conditions. As shown in Table 2, the recoveries are 94.0%, 101.7% and 103.6%, respectively and the concentrations of Cu^{2+} determined by the proposed ASS-ISE agree well with those obtained by AAS. Consequently, this PA@Ag/ASS-ISE could provide simple and accurate detection Cu^{2+} for environmental samples.

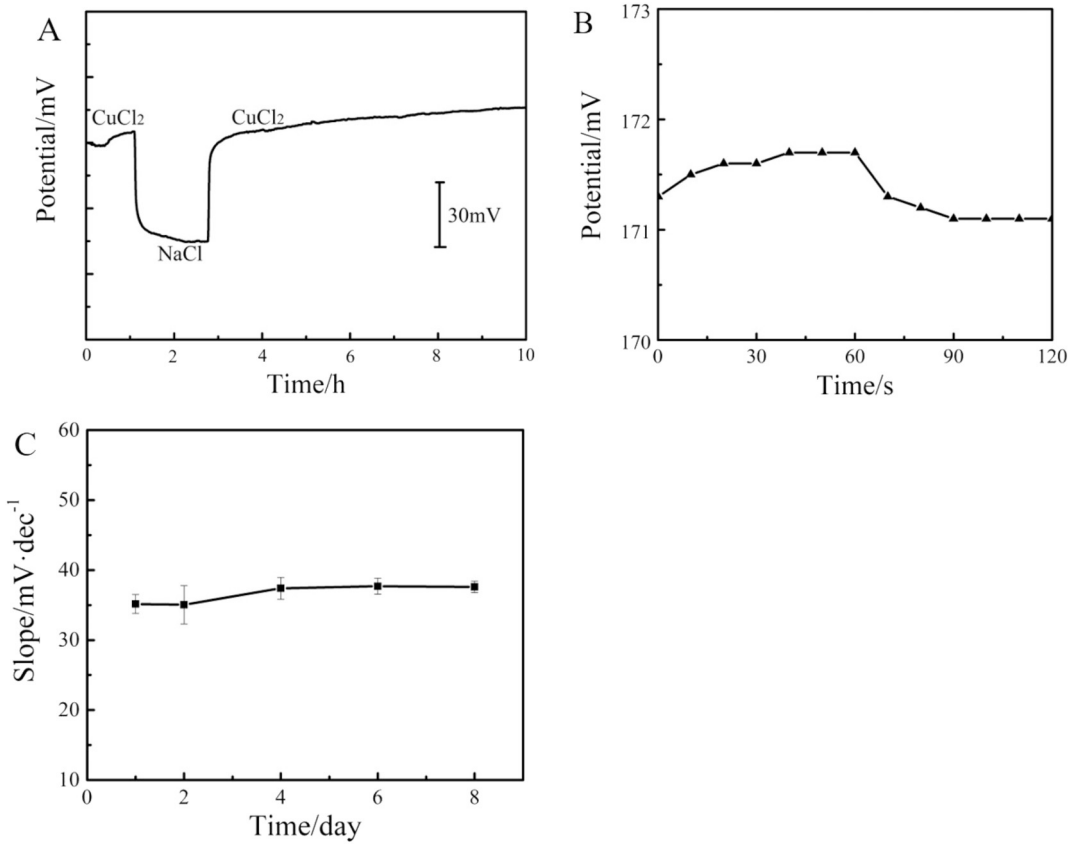

Fig. 6. (A) Water layer test for PA@Ag/ASS-ISE with the successive immersion into 10^{-4} M $CuCl_2$, 10^{-2} M NaCl and 10^{-4} M $CuCl_2$. (B) Chronopotentiometric response of PA@Ag/ASS-ISE in 10^{-5} M $CuCl_2$ with applying an anodic/cathodic current of 1 nA for 60 s. (C) Variation of slopes extracted from the potentiometric responses of PA@Ag/ASS-ISE during a period of 8 days.

4. Conclusions

In summary, a novel ASS-ISE based on PA@Ag was successfully developed and used for the potentiometric detection of Cu^{2+}. PA could display high affinity and selectivity towards Cu^{2+} and the presence of AgNPs could improve the conductivity and stability of the electrode. Under the optimum amount of PA@Ag, the fabricated PA@Ag/ASS-ISE presented a fast response with a slope of 31.3 ± 1.8 mV/dec in the linear range from 1.0×10^{-5} mol/L to 1.0×10^{-3} mol/L and a detection limit of 2.7×10^{-6} mol/L. With high selectivity towards the common metal ions and satisfactory stability, this electrode was exploited for the detection of Cu^{2+} in river samples and the results were validated by the AAS determinations, indicating the accuracy and precision of PA@Ag/ASS-ISE. Thus, this work provides a new strategy to develop ASS-ISEs for the detection of metal ions in environmental monitoring.

Urgency statement

Urgent publication is justified by the wonderful exhibition of Cu^{2+} detection in river water with a novel all-solid-state ion selective electrode based on PA@Ag. The strategy suggested in this work meets the needs of real-time environmental monitoring and is respected to show promising future in fast and continuous determination using open circuit potential.

Acknowledgements

This work was financially supported by the National Natural Science Foundation of China (Grant No. 21575042).

References

[1] R.W. Cattrall, H. Freiser, Coated wire ion-selective electrodes, Anal. Chem. 43 (13) (1971) 1905–1906.
[2] J. Bobacka, A. Ivaska, A. Lewenstam, Potentiometric ion sensors, Chem. Rev. 108 (2) (2008) 329–351.
[3] S.Q. Wang, Y.J. Wu, Gu Y, T. Li, H. Luo, L.H. Li, Y. Bai, L.L. Li, Y.D. Cao, H.Y. Ding, T. Zhang, Wearable sweatband sensor platform based on gold nanodendrite array as efficient solid contact of ion-selective electrode, Anal. Chem. 89 (19) (2017) 10224–10231.
[4] J.R. Sempionatto, R.K. Mishra, A. Martín, G.D. Tang, T.S. Nakagawa, X.L. Lu, A.S. Campbell, K.M.J. Lyu, J. Wang, Wearable ring-based sensing platform for detecting chemical threats, ACS Sens. 2 (10) (2017) 1531–1538.
[5] J.H. Guo, Uric acid monitoring with a smartphone as the electrochemical analyzer, Anal. Chem. 88 (24) (2016) 11986–11989.
[6] R.K. Mishra, L.J. Hubble, A. Martín, R. Kumar, A. Barfidokht, J. Kim, M.M. Musameh, I.L. Kyratizis, J. Wang, Wearable flexible and stretchable glove biosensor for on-site detection of organophosphorus chemical threats, ACS Sens. 2 (4) (2017) 553–561.
[7] W. Tang, Z. Wang, J. Yu, F. Zhang, P. He, Internal calibration potentiometric aptasensors for simultaneous detection of Hg^{2+}, Cd^{2+}, and As^{3+} based on a screen-printed carbon electrodes array, Anal. Chem. 90 (14) (2018) 8337–8344.
[8] W.J. Song, X.W. Wang, J.W. Ding, J. Zhang, W. Qin, Electrochemical sensing system for determination of heavy metals in seawater, Chin. J. Anal. Chem. 40 (5) (2012) 670–674.
[9] P. Bühlmann, E. Pretsch, E. Bakker, Carrier-based ion-selective electrodes and bulk optodes. 2. Ionophores for potentiometric and optical sensors, Chem. Rev. 98 (4) (1998) 1593–1688.
[10] C. Bieg, K. Fuchsberger, M. Stelzle, Introduction to polymer-based solid-contact ion-selective electrodes—basic concepts, practical considerations, and current research topics, Anal. Bioanal. Chem. 409 (1) (2017) 45–61.
[11] J. Hu, A. Stein, P. Bühlmann, Rational design of all-solid-state ion-selective electrodes and reference electrodes, TrAC Trends Anal. Chem. 76 (2016) 102–114.
[12] J. Li, T. Yin, W. Qin, An effective solid contact for an all-solid-state polymeric membrane Cd^{2+}-selective electrode: three-dimensional porous graphene-mesoporous platinum nanoparticle composite, Sensors Actuators B Chem. 239 (2017) 438–446.
[13] J. Ping, Y. Wang, Y. Ying, J. Wu, Application of electrochemically reduced graphene oxide on screen-printed ion-selective electrode, Anal. Chem. 84 (7) (2012) 3473–3479.
[14] M.K.A. El-Rahman, M.R. Rezk, A.M. Mahmoud, M.R. Elghobashy, Design of a stable solid-contact ion-selective electrode based on polyaniline nanoparticles as ion-to-electron transducer for application in process analytical technology as a real-time analyzer, Sensors Actuators B Chem. 208 (2015) 14–21.
[15] M. Guzinski, J.M. Jarvis, F. Perez, B.D. Pendley, E. Lindner, R.D. Marco, G.A. Crespo, R.G. Acres, R. Walker, J. Bishop, PEDOT (PSS) as solid contact for ion-selective electrodes: the influence of the PEDOT (PSS) film thickness on the equilibration times, Anal. Chem. 89 (6) (2017) 3508–3516.
[16] B. Paczosa-Bator, M. Pięk, R. Piech, Application of nanostructured TCNQ to potentiometric ion-selective K^+ and Na^+ electrodes, Anal. Chem. 87 (3) (2015) 1718–1725.
[17] E. Jaworska, M.L. Naitana, E. Stelmach, G. Pomarico, M. Wojciechowski, E. Bulska, K. Maksymiuk, R. Paolesse, A. Michalska, Introducing cobalt (II) porphyrin/cobalt (III) corrole containing transducers for improved potential reproducibility and performance of all-solid-state ion-selective electrodes, Anal. Chem. 89 (13) (2017) 7107–7114.
[18] Y. Yang, A.A. Ibrahim, P. Hashemi, J.L. Stockdill, Real-time, selective detection of copper (II) using ionophore-grafted carbon-fiber microelectrodes, Anal. Chem. 88 (14) (2016) 6962–6966.
[19] G. Jágerszki, A. Grün, I. Bitter, K. Tóth, R.E. Gyurcsányi, Ionophore–gold nanoparticle conjugates for Ag^+-selective sensors with nanomolar detection limit, Chem. Commun. 46 (4) (2010) 607–609.
[20] N. Wang, H. Dai, D. Wang, H. Ma, M. Lin, Determination of copper ions using a phytic acid/polypyrrole nanowires modified glassy carbon electrode, Mater. Sci. Eng. C 76 (2017) 139–143.
[21] F. Crea, C. De Stefano, D. Milea, S. Sammartano, Formation and stability of phytate complexes in solution, Coord. Chem. Rev. 252 (10 − 11) (2008) 1108–1120.
[22] C. Bretti, R.M. Cigala, C. De Stefano, G. Lando, D. Milea, S. Sammartano, On the interaction of phytate with proton and monocharged inorganic cations in different ionic media, and modeling of acid-base properties at low ionic strength, J. Chem. Thermodyn. 90 (2015) 51–58.
[23] Z. Li, G. He, B. Zhang, Y. Cao, Z. Jiang, T. Zhou, Enhanced proton conductivity of nafion hybrid membrane under different humidities by incorporating metal–organic frameworks with high phytic acid loading, ACS Appl. Mater. Interfaces 6 (12) (2014) 9799–9807.
[24] H. Wang, Z. Ma, Ultrasensitive amperometric detection of the tumor biomarker cytokeratin antigen using a hydrogel composite consisting of phytic acid, Pb (II) ions and gold nanoparticles, Microchim. Acta 184 (4) (2017) 1045–1050.
[25] Y. Liang, Y. Liu, X. Guo, P. Ye, Y. Wen, H. Yang, Phytate functionalized multi-walled carbon nanotubes modified electrode for determining trace Cu (II) using differential normal pulse anodic stripping voltammetry, Sensors Actuators B Chem. 201 (2014) 107–113.
[26] X. Gao, K. Lu, L. Xu, H. Xu, H. Lu, S. Hou, H. Ma, Excellent anti-corrosive pretreatment layer on iron substrate based on three-dimensional porous phytic acid/silane hybrid[J], Nanoscale 8 (3) (2016) 1555–1564.
[27] J. Li, T. Yin, W. Qin, An all-solid-state polymeric membrane Pb^{2+}-selective electrode with bimodal pore C_{60} as solid contact, Anal. Chim. Acta 876 (2015) 49–54.
[28] W. Qin, X. Fu R Liang, Q. Wang, T. Yin, W. Song, Trace-level potentiometric detection in the presence of a high electrolyte background, Anal. Chem. 84 (24) (2012) 10509–10513.
[29] B.P. Richard, E. Lindner, Recommendations for nomenclature of ion selective electrodes (IUPAC recommendations 1994), Pure Appl. Chem. 66 (12) (1994) 2527–2536.
[30] N.M. Tamin, R. Angel, Phytate phosphorus hydrolysis as influenced by dietary calcium and micro-mineral source in broiler diets, J. Agric. Food Chem. 51 (2003) 4687.
[31] T. Yin, Y. Liu, W. Qin, Single-piece solid-contact polymeric membrane ion-selective electrodes for silver ion, J. Electrochem. Soc. 160 (8) (2013) B91–B94.
[32] X. Zeng, S. Yu, Q. Yuan, W. Qin, Solid-contact K^+-selective electrode based on three-dimensional molybdenum sulfide nanoflowers as ion-to-electron transducer, Sensors Actuators B Chem. 234 (2016) 80–83.
[33] J. Bobacka, Potential stability of all-solid-state ion-selective electrodes using conducting polymers as ion-to-electron transducers, Anal. Chem. 71 (21) (1999) 4932–4937.
[34] P. Enrique, F.X. Rius, P. Blondeau, A potassium sensor based on non-covalent functionalization of multi-walled carbon nanotubes, Analyst 138 (9) (2013) 2698–2703.